

Liquid-like instabilities in gold nanowires fabricated by focused ion beam lithography

J. P. Naik,^{1,a)} K. Das,^{2,a)} P. D. Prewett,¹ A. K. Raychaudhuri,² and Yifang Chen³

¹*School of Mechanical Engineering, University of Birmingham, Birmingham B15 2TT, United Kingdom*

²*Centre for Nanotechnology, S N Bose National Centre for Basic Sciences, Salt Lake (Sector-III), Kolkata 700098, India*

³*STFC-Rutherford Appleton Laboratory, Chilton, Didcot OX11 0QX, United Kingdom*

Observation of liquid-like instabilities is reported in Au nanowires formed by nanopatterning of Au films using focused ion beam (FIB) on different types of Si substrates including those passivated with SiO₂ or Si₃N₄ surfaces. The onset of the instability, which can ultimately lead to break up of the FIB patterned nanowires into gold islands, occurs when the diameter of the nanowire is below a critical range, which depends on the conductivity of the substrate and the extent of native oxide present on it. We also observe the formation of Taylor cones on very narrow nanowires grown on insulating substrates at the onset of instabilities. This effect is further strong evidence of liquid behaviour and is the result of charging of the wires during FIB nanofabrication.

There is considerable interest in conducting nanowires because of their importance in the study of nanoscale structures and their use in nanoscale devices including nanoelectromechanical systems (NEMS) and nanoelectronics.^{1,2} In order to use metallic nanowires in these applications, for example as interconnects, they must have well defined stable geometries. NEMS devices are most frequently made using silicon microfabrication technology so it is important to study the fabrication of conducting nanowires on silicon or related substrates like SiO₂/Si or Si₃N₄/Si to develop robust methods for producing them under varying surface conditions and to ensure that they are ultimately manufacturable.³ Focused ion beam (FIB) is an important tool for rapid prototyping of nanoscale devices and the work reported here presents results of using FIB as a lithography tool to produce gold nanowires on technically important surfaces in order to study the structural integrity of these nanowires as a function of their width and substrate surface conditions. We show that, below a certain width, the fabrication methods can lead to liquid-like instabilities in the FIB patterned nanowires. These instabilities depend *inter alia* on the electrical conductivity of the substrate and the nature of its surface passivation. We find that metal lines on more conducting substrates can be patterned using FIB to much smaller widths before the instabilities set in. The effect of charge accumulation during the fabrication process, particularly on insulating substrates, can also lead to the formation of Taylor cones,⁴ which are clear signatures of the liquid-like behaviour dominated by surface energy.

It has previously been observed that nanowires with small lateral dimensions may show instabilities which lead to their break up into small spheres.⁵ Even nanowires grown by electrochemical deposition and constrained by templates⁶ show fluctuations in diameter, which can be detected by high precision resistance measurements. These phenomena, which

are of significant concern to the nanotechnology community, have been attributed to the Rayleigh-Plateau instability⁵⁻⁸ that occurs in liquid columns with large aspect ratio due to surface energy effects. Initial experiments to form gold nanowires on silicon substrates by FIB patterning have also revealed these effects⁹ and have stimulated the more detailed study reported here. Most of the studies to date were done on freestanding nanowires grown inside the templates,¹⁰⁻¹² whereas surface deposited nanowires produced by top-down lithography of various kinds are of greater relevance for interconnects in nanotechnology. This motivated the present work on liquid instabilities in gold nanowires fabricated by nanopatterning physical vapour deposited films using FIB. The important finding of this paper is that the physical characteristics of the substrate (resistivity, adhesion of the film, etc.) play an important role in deciding the minimum width of the nanowire that can be patterned using FIB.

A nanowire can be approximated as a cylinder. When liquid-like instabilities originating from surface tension sets in such nanowires of the Rayleigh-Plateau type,^{7,8} it leads to modulation in the diameter with wavelength λ which is larger than the circumference. Generally, for a wire of unperturbed radius of cross-section r_0 supporting a volume-conserving fluctuation with wave vector $k = \frac{2\pi}{\lambda}$ in the z -direction, the radius of the wire at a distance z along its axis is given by⁶

$$r(z) = r_0 + b \sin\left(\frac{2\pi}{\lambda}z\right), \quad (1)$$

where b is the perturbation amplitude. When $\lambda \geq 2\pi r_0$, the wire will break up under surface tension stress, as in the case of the Rayleigh instability of a column of liquid^{7,8} when the radius r_0 falls below $r_{\min} = \frac{S}{\sigma_Y}$, where S is the surface tension and σ_Y is the yield strength. For Au with $\sigma_Y \approx 100$ MPa and $S \approx 1.3$ N/m,¹³ $r_{\min} \approx 13$ nm, predicting that liquid instabilities may be expected for Au nanowires with lateral dimension of a few tens of nm. While the above analysis for

^{a)}J. P. Naik and K. Das contributed equally to this work.

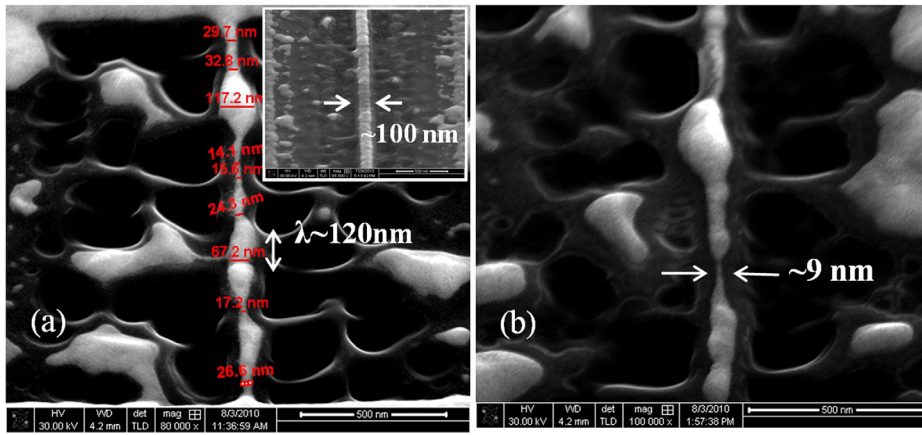


FIG. 1. SEM image of instability in thin gold nanowire (sample A) on (a) lightly doped Si with native oxide (inset shows no instability for thicker wires of diameter ~ 100 nm). (b) Instability seen on passivated lightly doped Si.

a free-standing nanowire depends only on the material parameters, the exact value of r_{min} for the case of a nanowire on a substrate will be determined by the effective value of S on the substrate and any instability due to charging of the film during patterning together with wire-to-surface adhesion parameters. The present investigation shows that this is indeed the case for nano-patterned Au lines. In particular, factors arising from charging do play a role, as demonstrated below by varying the substrate conductivity.

50 nm thick Au films (with 4 nm thick Cr adhesion layer) were deposited in high vacuum on three different silicon substrates. The nanowires were fabricated by sputtering away the gold film from both sides using Ga^+ ions in an FEI Helios 600 Dual Beam system with a beam current ~ 30 pA at energy of 30 keV. The nanowires produced in this way have approximately rectangular cross-section with widths ranging from more than 200 nm down to 10 nm; their length in each case is $2 \mu\text{m}$. Scanning electron microscopy (SEM) of the nanowires using a field emission gun was done *in situ*, immediately following fabrication. To investigate the effect of charging, we carried out experiments on Si (100) with different doping levels: one with light p type doping (resistivity $\rho \sim 5 \Omega \text{ cm}$) marked as sample A and one with heavily doped p type (resistivity $\rho \sim 0.01 \Omega \text{ cm}$) marked as B. Both substrates A and B have native oxide of thickness ~ 4 nm. To make the substrates more resistive, we used Si (100) with 300 nm thermally grown SiO_2 (sample C) and one with 200 nm Si_3N_4 on (100) Si (sample D). The resistivity of sample C is the largest followed by that of sample D, sample A, and sample B.

To investigate the effect of surface passivation of the substrates (which can control the wetting), experiments were conducted using Si (100) substrates treated with buffered hydrofluoric acid (HF) for both lightly and heavily doped substrates, marked as samples “passivated A” and “passivated B,” respectively.

After patterning by Ga^+ ions, a line scan energy-dispersive x-ray (EDX) measurement was carried out across the width of each gold nanowire along the width to reveal atomic distributions. The Ga contamination was found to be localized near the outer edges of the wire, where the effects of the ion beam milling are concentrated with some limited spread into the nanowire due to the non Gaussian tails on the focused ion beam.¹⁴ The EDX data are given in supplementary S1.¹⁵ Because of the FIB etch method employed, beam induced heating is confined to the edges of the nanowire and, therefore, does not play a significant role in the observed instabilities.

The patterning studies were done on nanowires with starting width ~ 300 nm. The FIB-patterned nanowire of width 100 nm on substrate A ($\rho \sim 5 \Omega \text{ cm}$) is shown in the inset of Fig. 1(a). This is the typical view of all the nanowires grown on different substrates with width 100 nm and shows no modulation in width. However, on thinning the wire to less than 60 nm, the diameter modulation sets in, as shown in Fig. 1(a), leading to a disordered wavy structure with accumulated nearly spherical regions of diameter 100 nm, created by flow. The presence of spherical regions strongly suggests the creation of liquid-like instabilities. The narrowest wire that can be made with extreme modulation has a nominal width ~ 15 nm as shown in Fig. 1(a). The wavelength of

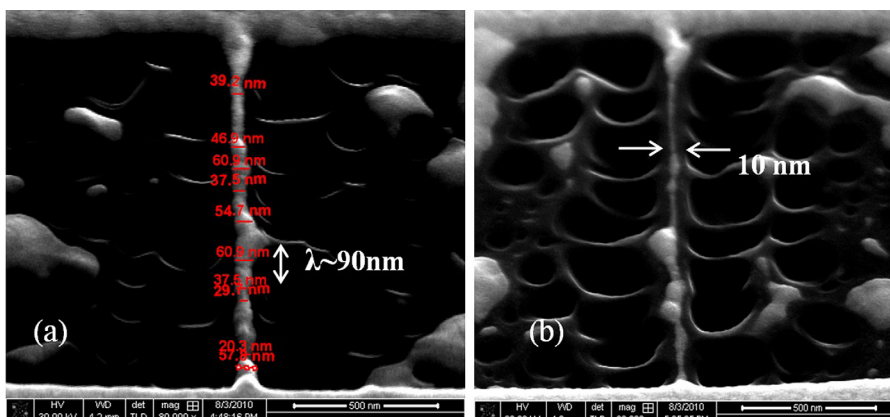


FIG. 2. (sample B) (a) Au nanowire ~ 40 nm wide fabricated on unpassivated highly doped Si, (b) thin straight nanowire with limited instability fabricated on passivated highly doped Si.

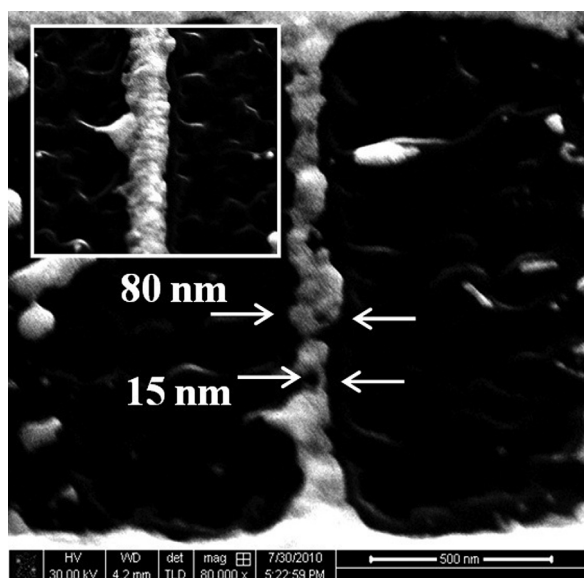


FIG. 3. SEM image of Au nanowires fabricated on (a) SiO_2 (300 nm)/Si (sample C) showing more pronounced liquid-like instability. (inset showing evidence of Taylor cone formation with apex jetting).

modulation λ is around ~ 120 nm. For passivated sample A, the observations are qualitatively the same. In this case, the wire does not fragment completely into spheres and connected nanowires are seen down to a width of ~ 9 – 10 nm (Fig. 1(b)) albeit with much smaller length (marked by arrow in Fig. 1(b)).

Fig. 2 shows the results for a Au wire fabricated on unpassivated and passivated substrate B which has very low resistivity, $\rho \sim 0.01 \Omega \text{ cm}$. Thinner wires can be patterned before break-up, in marked contrast to the previous lightly doped cases. Fig. 2(a) shows a wire of about 50 nm diameter with a small radial variation. The wavelength of modulation is $\lambda \sim 90$ nm. This was then further thinned down to achieve a wire of minimum width of ~ 8 nm, having connected spheres of diameter ~ 30 nm in an extended “peanut” shape. The passivation of the surface leads to a relatively long ($\sim 1 \mu\text{m}$) uniform wire of diameter ~ 10 nm as shown in Fig. 2(b). Thus, from both samples A and B, it is seen that surface passivation leads to the formation of wires with considerably smaller width.

The results demonstrate a noticeable change in the stability of the wire depending on the resistivity of the Si sur-

face, which can be controlled by doping of the substrates, and on the presence of different native oxide layers, presumably because charging is reduced while using highly doped substrates. Removal of the native oxide from the substrate also contributes to improved stability through better adhesion due to silicon dangling bonds.

In order to investigate further the effects of substrate conductivity and charging effects on the patterned nanowire stability, the experiments were repeated for two further substrates C and D. Fig. 3 shows the results for the sample C ($300 \text{ nm SiO}_2/\text{Si}$). The liquid instabilities are apparent even for the wider wires in this case. In addition, for substrates with lower conductivity, the charging due to the FIB process leads to the formation of Taylor cones⁴ on the sides of the nanowire. A magnified image of the Taylor cone is shown in the inset of Fig. 3 and is strong evidence of liquid behaviour. The results for sample D ($200 \text{ nm Si}_3\text{N}_4/\text{Si}$ substrate) are similar to those for sample C, as seen in Fig. 4(a). The enhancement of the surface resistivity and inhibition of the charge flow lead to greater distortions in the patterns for samples C and D. In Fig. 4(a), the instability of the wire becomes more prominent, with thinning to regions in which spherical “beads” of radius 40 nm are just connected through regions of ~ 15 nm width. The wavelength derived from the SEM image is found to be $\lambda \sim 75$ nm (as marked in Fig. 4(a)), which is more than the circumference, consistent with Rayleigh’s theory.⁴ Finally, the liquid-like instability causes the wire to fragment into nanoparticles of size ~ 100 nm diameter spaced by ~ 100 nm shown in Fig. 4(b). The appearance of instabilities with an associated wavelength is a signature of liquid-like behaviour and this is observed in all cases studied. However, the wavelength λ depends on the substrate as well as on details of the surface passivation. A summary of data for the Rayleigh liquid instability extracted from the SEM pictures is given in Table I. The critical diameter for each case is also shown in the table. Here, we find the λ/d value to be less than the expected value of ~ 3 predicted by the Rayleigh-Plateau model of falling liquid. This is almost certainly due to the modification of the nanowire by its interface with the supporting surface where adhesion plays a major role. The critical diameter is found to be in the range of 10–20 nm, lowest for highly doped Si and maximum for SiO_2 , which have, respectively, the lowest and highest resistivities of the four different samples studied.

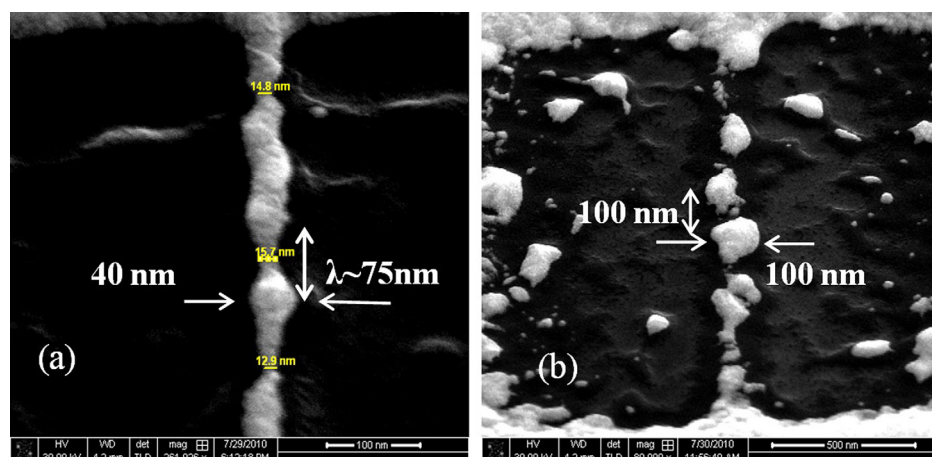


FIG. 4. (a) Nanowire on Si_3N_4 (200 nm)/Si (sample D) at the onset of fragmentation. (b) Nanowire fragmented into spheres.

TABLE I. Properties of the nanowire instability for different substrates.

Substrate	Resistivity (Ω cm)	Average diameter, d (nm)	Average wavelength, λ (nm)	λ/d	Smallest diameter obtained (nm)
Un-passivated low doped Si (sample A)	5×10^1	65	120	1.8	14
Passivated low doped Si (sample A)	5×10^1	50	90	1.8	10
Un-passivated highly doped Si (sample B)	1×10^{-2}	55	90	1.7	8
Passivated highly doped Si (sample B)	1×10^{-2}	55	80	1.5	10
Si ₃ N ₄ (sample D)	1×10^{14}	35	75	2.2	13
SiO ₂ (sample C)	10^{14} – 10^{16}	80	140	1.8	15

To summarize, we have investigated the structural and morphological stabilities of Au nanowires, fabricated by focused ion beam etch of gold films on different substrates. It is shown that, even in the presence of good surface adhesion, there is an onset of liquid-like instabilities when the diameter of the nanowires falls below a critical range. The stability of the wires is noticeably better in the case of conducting Si substrates than for silicon coated with the insulators like SiO₂ or Si₃N₄. This is attributed to the greater conductivity of Si, which minimizes space charge effects during FIB fabrication. The buffer HF treatment of Si to remove the native oxide from the surface gives improved resistance to instability due to the much improved adhesion of the gold film. The instabilities investigated in this study could severely limit the use of FIB patterned gold nanowires in nanosensors and other nanoscale devices. The instabilities can ultimately lead to break up of the nanowires into islands of metal and are clearly of the Rayleigh-plateau type. On insulating substrates, there is also clear evidence of electrohydrodynamically formed Taylor cones that form due to charging during patterning by FIB.

This work was carried out under UKIERI, a joint programme between the Department of Science and Technology (DST), Government of India and the British Council of the

UK Foreign Office. Work of K.D. and A.K.R. and the funding for the Helios 600 were supported by DST sponsored project on Centre for Nanotechnology.

¹M. C. Petty, *Molecular Electronics* (Wiley-VCH, Weinheim, 2007).

²E. Mooij and Yu. Nazarov, *Nat. Phys.* **2**, 169 (2006).

³M. J. Kelly, *Nanotechnology* **22**, 245303 (2011).

⁴G. I. Taylor, *Proc. R. Soc. London, Ser. A* **280**, 383 (1964).

⁵F. A. Nichols and W. W. Mullins, *Trans. Metall. Soc. AIME* **233**, 1840 (1965).

⁶A. Bid, A. Bora, and A. K. Raychaudhuri, *Phys. Rev. B* **72**, 113415 (2005).

⁷J. Plateau, *Experimental and Theoretical Statics of Liquids Subject to Molecular Forces Only* (Gauthier-Villars, 1873).

⁸L. Rayleigh, *Proc. London Math. Soc.* **S1-10**, 4 (1878).

⁹J. P. Naik, P. D. Prewett, K. Das, and A. K. Raychaudhuri, *Microelectron. Eng.* **88**, 2840 (2011).

¹⁰E. Toimil-Molares, A. G. Balogh, T. W. Cornelius, R. Neumann, and C. Trautmann, *Appl. Phys. Lett.* **85**, 5337 (2004).

¹¹S. Karim, M. E. Toimil-Molares, A. G. Balogh, W. Ensinger, T. W. Cornelius, E. U. Khan, and R. Neumann, *Nanotechnology* **17**, 5954 (2006).

¹²Y. Qin, S.-M. Lee, A. Pan, U. Gosele, and M. Knez, *Nano Lett.* **8**, 114 (2008).

¹³C. H. Zhang, F. Kassubek, and C. A. Stafford, *Phys. Rev. B* **68**, 165414 (2003).

¹⁴C. Lehrer, L. Frey, S. Petersen, and H. Ryssel, *J. Vac. Sci. Technol. B* **19**, 2533 (2001).

¹⁵See supplementary material at <http://dx.doi.org/10.1063/1.4761249> for line scan EDX measurement.